THE SOFT AND MEDIUM–ENERGY X–RAY VARIABILITY OF NGC 5548: A REANALYSIS OF EXOSAT OBSERVATIONS

G. Tagliaferri

Osservatorio Astronomico di Brera, V. E. Bianchi 46, 22055 Merate (Lc), Italy

e–mail: gtagliaf@antares.merate.mi.astro.it

G. Bao[1] , G. L. Israel[2]

International School for Advanced Studies (SISSA), V. Beirut 2–4, 34013 Trieste, Italy

e–mail: Bao.gang@avh.unit.no — gianluca@vega.sissa.it

L. Stella[2,3]

Osservatorio Astronomico di Brera, V. E. Bianchi 46, 22055 Merate (Lc), Italy

e–mail: stella@antares.merate.mi.astro.it

A. Treves

International School for Advanced Studies (SISSA), V. Beirut 2–4, 34013 Trieste, Italy

e–mail: treves@tsmi19.sissa.it

ABSTRACT

We present a detailed cross–correlation (CCF) and power spectrum re–analysis of the X–ray light curves of the bright Seyfert 1 galaxy NGC5548 obtained with *EXOSAT*. The 0.05–2 keV and 1–4 keV light curves are cross–correlated with the 1–9 keV and 4–9 keV light curves respectively. We discuss how spurious time lags can be introduced by systematic effects related to detector swapping as well as the switching on and off of the instruments. We also find strong evidence that one of the ME detectors was not working normally during the second part of the March 1986 observation. When these effects are taken into account, the CCF peaks are in all cases consistent with the absence of delays

---

[1]Current address: Physics Institute, University of Trondheim, N–7055 Dragvoll, Norway

[2]Affiliated to the International Center for Relativistic Astrophysics

[3]Now at the Astronomical Observatory of Rome, Via dell'Osservatorio 2, 00040 Monteporzio Catone, Roma

between X–ray variations at different energies. This is unlike the results found by several authors based on the same data.

The power spectra of the 1–9 keV light curves are calculated and a detailed search for quasi periodic oscillations (QPOs) carried out on these spectra by using a new technique for the detection of periodic (or quasi–periodic) signals even in the presence of source noise variability. No significant peaks are found above the 95% confidence detection threshold, except during the second part of the March 1986 observation, most probably as a consequence of the ME detector malfunctioning. We discuss and compare our results with those of Papadakis & Lawrence (1993a).

Subject headings: Seyfert objects — galaxies: individual (NGC5548) — X–rays: sources

1. Introduction

NGC5548 is a bright, close–by (z=0.017) Seyfert 1 galaxy which was extensively studied in different bands of the electromagnetic spectrum. Large variability of both lines (optical–UV) and continuum have been reported making the source an important laboratory for exploring the mechanisms of spectral formation in AGNs. In particular the study of correlations and time lags between the various spectral components represent an important technique for constraining the geometry of the emitting regions (e.g. Mushotzky et al. 1993, and references therein). ¿From a systematic study of IUE spectra (1200–3000 Å Clavel et al. 1991) a strong correlation between emission lines and continuum variability was established, with lines responding to the continuum variations with delays of 10–70 days, depending on the degree of ionization of the species (a higher ionization corresponds to a smaller delay). Systematic UV–X–ray observations indicated a strong correlation in the continuum variability in the two bands with un upper limit of ≤ 6 days to any delay (Clavel et al. 1992). This, together with the simultaneous optical UV continuum variations, showed that at least a component of the optical–UV continuum should be generated by reprocessing of the X–rays, rather than by the intrinsic disk variability, which should be characterized by longer time–scales (Molendi, Maraschi & Stella 1992). ROSAT observations of a soft X–ray flare with correlated variability in the UV, but without a corresponding change in higher energy X–rays (Done et al. 1995, Walter et al. 1995) made apparent the complexity of the processes occurring in the object. New simultaneous observations at various wavelengths are currently being analysed (e.g. Korista et al. 1995 and references therein).

The importance of reprocessing on both cold and warm material is confirmed by the observation of a Fe K fluorescent line at a centroid energy of ~ 6.4 keV , and of a Fe absorption edge at ~ 8 keV superimposed to a rather complex continuum (Nandra et al. 1991). This rich observational scenario may be accounted for by models where a hot corona above the accretion disk provides the hard X–ray photons. At the same time these photons are in part reprocessed by an accretion disk which in turn generates the photons for the Compton cooling of the electrons in the hot corona (e.g. Haardt & Maraschi 1993, Życki et al. 1994).

Because of its ~ 4 day orbital period, allowing long uninterrupted exposures and its wide spectral range (0.05–10 keV), the EXOSAT satellite was particular apt to study variability and reprocessing in the X–ray band on time scales of tens of hours or less. For a systematic study of the variability of Seyferts and QSO contained in the EXOSAT database we refer to Grandi et al. (1992) and Green, Mc Hardy & Lehto (1993).

NGC 5548 was observed with EXOSAT 12 times in 1984–86 with a total

exposure of $\sim$200 hrs. Flux variations up to a factor of 4 and 3 between the various observations and within each observation, respectively, were clearly seen. A detailed analysis of the EXOSAT light curves was performed by several authors. Variability on timescales of hours was studied by Kaastra & Barr (1989, hereafter KB), who searched for delays between variations in the soft (0.05–2 keV) and medium (2–6 keV) energy X–ray light curves, suggesting that soft X–rays variations lead by $\sim 4600 \pm 1200$ s. This result, if confirmed, would have profound theoretical implications, favoring models, such as those mentioned above, where the medium energy X–rays are produced by Compton scattering off the UV/soft X–ray photons by electrons in a hot corona. Walter and Courvoisier (1990) re–examined the same data by using a different analysis technique substantially confirming the results of KB.

Papadakis & Lawrence (1993a, hereafter PL) performed a power spectrum analysis the EXOSAT ME light curves and reported the likely detection of quasi–periodic oscillations (QPOs) in 5 out of 8 observations. They suggested that the frequency ($\sim$2 mHz) of the QPOs increases with source intensity, whereas the fractional root mean square amplitude of variability decreases as the source brightens. Since this behaviour is similar to that of e.g. compact galactic X–ray binaries, PL suggest that intensity–correlated QPOs in NGC5548 may also arise from instability or variability in an accretion disk around a massive black hole.

Because of the quality of the EXOSAT light curves and the importance of the physical inferences derived from them, we feel justified in presenting a new and independent analysis of relatively old data. This is done in the light of some systematic uncertainties which may arise in the analysis of the EXOSAT light curves from relatively faint sources (such as most AGNs). These uncertainties are discussed in greater detail in a paper on the BL Lac object PKS 2155–304 (Tagliaferri et al. 1991, hereafter Paper I).

In Section 2.1 we summarise the characteristics of the EXOSAT light curves of NGC5548. Our CCF analysis for different X–ray energy bands is described in Section 2.2. Details on our search for QPOs are given in section 2.3. The conclusions are in Section 3.

2.   Data Analysis

2.1.   Light Curves

The data considered here have been obtained through the EXOSAT database and refer to the low energy imaging telescope (LE) and the medium energy experiment (ME) (White & Peacock 1988). The Argon chambers of the ME experiment consisted of an array of 8 collimated proportional counters mainly sensitive to 1–20 keV X–rays. In order to monitor the background rates and spectrum the ME was generally operated with half of the detector array pointed at the target, and half at a nearby source–free region. The two halves were usually interchanged every 3–4 hours, a procedure indicated as *array swap* (hereafter *AS*). The LE telescope was used with a Channel Multiplier Array (CMA) in the focal plane. The CMA was sensitive to the 0.05–2.0 keV energy band and had no intrinsic energy resolution (De Korte et al. 1981); however, a set of filters with different spectral transmission could be interposed in front of the detector.

The EXOSAT observations of NGC 5548 considered here are summarised in Table 1. Column 1 gives a letter identifying each observation, column 2 the observing date, column 3 the ME exposure time, column 4 the number of *AS*, column 5 the r.m.s. dispersion calculated from the 1-9 keV light curves with a binning time of 1000 s, column 6 the expected r.m.s. dispersion from counting statistics and column 7 the average 1–9 keV ME count rate (per ME array half). Columns 8 through 10 give the exposure times in the LE telescope used in conjunction with the Aluminium/Parylene (Al/P), Boron (Bor) and thin–Lexan (3Lex) filters, respectively. The ME data products (energy spectra and light curves) stored in the EXOSAT database have been given a quality flag ranging from 0 (unusable) to 5 (excellent). Data with quality flag between 3 and 5 are of sufficiently good quality for a detailed analysis (see *The EXOSAT Database System: available databases* (1991)). In our analysis we have considered all observations with the ME quality factor ≥ 3; this excludes two observations carried out in March 1984 and January 1985 (not listed in Table 1) with exposure times of ~ 36000 and ~ 22000 s, respectively. An example of light curves is shown in Fig. 1.

2.2. Cross Correlation Analysis

In order to study the possible delays between the intensity variations in the various bands we calculated the CCF of the LE (0.05–2 keV) and ME light curves (1–9 keV); this is indicated as LE/ME. For the LE we considered only the light curves that were obtained with the 3Lex filter (which provided the highest photon throughput) and were longer than ~ 15000 s. This allows to search for delays longer than one hour. Observations I and J are the only suitable for the LE/ME analysis. We have also cross–correlated the 1–4 keV to the 4–9 keV ME light curves

(ME/ME): This subdivision of the ME range for NGC 5548 provides comparable count rates in the two bands. The ME/ME CCF analysis was also performed for all the other observations given in Table 1. We used the standard CCF algorithm contained in the timing analysis package *Xronos* (Stella & Angelini 1992), which is well suited for equispaced and (nearly) continuous data, such as the EXOSAT light curves of NGC 5548.

In the analysis of the EXOSAT light curves of PKS 2155–304 (Paper I) we identified a number of systematic effects that may alter the CCF. These are briefly summarized here. A possible problem is related to the AS procedure, which leaves an uncertainty of up to ± 0.5 cts s^{-1} in the level of the background subtraction. If the results of the CCF analysis change significantly by adding or subtracting one of the light curves across the AS with a constant value of up to 0.5 cts s^{-1}, then these results should be considered with caution.[1] Moreover, the presence of AS implies that the ME light curves are interrupted by gaps of typical duration of 15 minutes. Although these durations are short compared to the entire light curves, the discontinuity that they introduce in the ME light curves can have strong effects on the CCF. To reduce the effects of the gaps, we fill them with the running average of the light curve calculated over a duration of ~ 1.5 hour. With this choice the moving average follows the light curve behaviour on time scales of hours, while the statistical fluctuations are reduced due to the relatively high number of points used in the average. For a given observation, the start and end times of the LE and ME light curves usually differ from a few minutes to tens of minutes. This can alter the shape of the CCF, especially if standard algorithms are used as in our case (see Paper I). To avoid the problem altogether one should therefore make sure that the two light curves are strictly simultaneous, disregarding the data intervals in which only one light curve is available.

In our analysis we rebinned the light curves in time bins of 1000 s. We excluded all bins with an exposure time of less than 50% . In some cases we used also intensity windows in order to exclude those bins in the original light curves (resolution of 4–10 s) which were clearly affected by an inadequate background subtraction.

The CCF analysis of observation J, the longest and that for which KB report delays between soft and hard variations, was performed in two different ways both for the ME/LE and ME/ME cases. First we considered the entire LE and ME light curves (see Fig. 1), with the gaps bridged with the running mean and did not exclude the non-simultaneous parts of the light curves. A ~ 6 hr interruption is apparent close to the beginning of the observation, due to the switch off of the EXOSAT

---

[1]Due to a misprint, paper I reports an uncertainty of up to ± 0.05 cts s^{-1} the correct value is the one reported here (Parmar & Izzo 1986; A.N. Parmar, private communication).

instruments at the perigee passage (see Fig. 1). If the ~ 1.5 hr long light curve interval that preceeds this long gap, is included in the analysis, than the LE/ME CCF shows a marked asymmetric peak centered around a delay of $\sim 7000 - 8000$ (Fig. 2). If we exclude the gap or impose the simultaneity of the two light curves, then the delay is much shorter or not present at all. We note that the light curve shown in Fig. 2 of KB paper not only includes the gap, but in the LE it includes another 30 ks of data at the end of the NGC 5548 observation, when this source was seen serendipitously in the field of the BL Lac object 1E1415.6-2557 (Giommi et al. 1987). Of course there are no ME data for this additional interval. It appears that for their timing analysis KB used all the data shown in their Fig. 2, altough this is not explicitly stated. As we have shown the non simultaneity of the two data sets strongly affects the results of CCF analysis (see also paper I). Therefore, we did not consider the extra LE data on NGC 5548 during the EXOSAT observation of 1E1415.6-2557. Moreover, in the rest of all our analysis we considered only strictly simultaneous data. We then also excluded the first ~ 7.5 hr from our analysis of the light curves of observation J. The LE/ME and ME/ME CCFs calculated in this way are shown in Fig. 3. A peak is clearly present in the CCFs which is in both cases asymmetric and centered near zero time delay. To derive quantitative information on possible delays between the variations in the soft and hard X–ray light curves, we fitted the central peak of the CCF with a Gaussian function plus a constant. In the case of the ME/ME CCF, a linear term was added to the fit, to account for the stronger asymmetry of the CCF (see Fig. 3). The results for centroid of the peak are $+400$ s (90% confidence interval: $-800 + 1500$ s) and $+1500$ s ($+500 + 2700$ s) respectively.

The second procedure consisted in dividing the light curve into three segments, the first two segments, about 6 and 7 hour long, containing only one AS, and the third segment, of about 11 hours, containing two AS. The CCF was calculated for each segment. This treatment reduced the possible effects of the AS discontinuity on the CCF; however it has the disadvantage of decreasing the longest detectable delay time (about 2–3 hours, a value still consistent with the delay time reported by KB). There is essentially no peak in the second intervals both for the LE/ME and ME/ME CCFs, while in the first interval in both CCFs there is a weak peak centered on zero time delay (Figs 4a–d). In the third segment a clear peak is present in the ME/ME CCF, while a feature with a negative and a positive component can be noted in the LE/ME CCF (Figs 4e,f). This feature is due to the presence of the two AS, indeed if we consider only one of the two AS each time, then the first AS gives rise only the negative peak, whereas the second AS causes only the positive peak. Moreover, by looking at the ME light curves it seems that the central parts (between the two AS, see fig 5) are not properly aligned with the other two. We tested how stable the CCF peaks are to the addition of a constant value to the central parts.

For instance in the ME/ME CCF the peak disappears completely by adding 0.1 and 0.4 cts s^{-1} to the central 1–4 and 4–9 keV light curves respectively (Figs 5a,b shows the two ME light curves before and after having added the above constant values to the central part). As a further test we performed an LE/ME and an ME/ME CCF analysis by considering only the first 13 hrs of this observations (i.e. 3 AS). Again no peak is present in either CCF. We can conclude that the segmented analysis does not provide evidence for delays between the LE/ME and ME/ME variations.

Another problem emerged through a careful inspection of the ME light curves (Figs 1 and 5). One can see that the light curve intervals between the fourth and fifth AS and after the sixth AS are much noisier than the others (this is seen even more clearly in light curves with a somewhat shorter binning time). This is probably due to one of the three aligned detectors (first half of the ME in this case) not behaving normally. That this behaviour arises from one of the detectors (and not from the source) is confirmed both by the lac of it in the LE light curve and by the fact that between the fifth and sixth array swap, when the relevant half of the ME array is offset, one of the detectors (detector B as reported in the "ME Obervation Log book" A. Parmar, private comunication) was switched off, due to malfunctioning. After the sixth array swap detector B was switched on again, but it was clearly not functioning properly, yet (see Figs 1 and 5). In this case the malfunctioning detector should be excluded from the analysis, something that was not done in the automatic analysis that generated the ME database products for this observation. We conclude that detector B in the first ME half is most likely responsible for the extra variability in the ME light curves. We intended to repeat the analysis starting from the ME raw data. However we could not obtain the original data from ESA, since the relevant magnetic tape turned out to be unreadable (A. Parmar, private communication).

For all other observations in Table 1, because of the shorter exposure times and therefore lower number of AS (see Tab. 1), we considered the cross correlation of the entire light curves with the data gaps bridged by the running mean. For observation I, the second longest, the LE/ME CCF is again flat, while the ME/ME CCF shows a strong peak centered around zero time delay (Fig 6). It can be seen from the figure, however, that the *half width at half maximum* of this peak is comparable to the duration of the light curve segments between AS; this suggests that the peak might be due to the systematic uncertainties in the ME background subtraction across the AS. To test the reliability of this CCF peak we subtracted 0.2 *cts s^{-1}* to the first part of both ME (1–4 and 4–9 keV) light curves (before the first AS) and added 0.2 *cts s^{-1}* to the second and third parts of the 4–9 keV light curve, trying to reduce the discontinuity due to AS visible in the light curves. Again this was sufficient to make the CCF peak disappear. Various other tests showed that by adding or subtracting 0.1–0.2 *cts s^{-1}* (which are well within the systematic uncertainties of the detector background subtraction) to selected segments of the ME light curves in between

AS, the peak can become more pronounced or disappear altogether. Also the r.m.s. dispersion is clearly affected by the *AS*; indeed if we add 0.3 and 0.5 *cts s*$^{-1}$ to the 1-9 keV light curve before the first and after the last *AS*, the resulting r.m.s. dispersion is 0.28 to be compared with the value of 0.39 given in Table 1.

For all other observations, we calculated only the ME/ME CCF. No peak was detected in the CCFs of observations A, C, D, E, F and H, consistent with the fact that no significant variability is present in the 1-9 keV light curves (see Table 1). Instead a clear peak was detected in observations B and G (Figs 7,8). In both cases the peak is not centered around zero delay. This would indicate that the variations in the 1–4 keV light curves precede the variations in the 4–9 keV light curve by about 2000–3000 s. However, we believe that also these delays are spurious. In the case of observation G the peak is almost certainly due to background subtraction uncertainties across the *AS*. Fig. 9a gives the original ME light curves, while Fig. 9b shows the same light curves after the addition of a constant value of 0.2 cts s^{-1} to the segments before the *AS*. The latter light curves show virtually no discontinuity across the *AS* and the resulting CCF is flat. Again by adding 0.5 *cts s*$^{-1}$ to the 1-9 keV light curve before the *AS*, the resulting r.m.s. dispersion is 0.18 to be compared with 0.34 of Table 1. We also used observation G to test whether the abrupt discontinuity introduced by the *AS* can cause the asymmetry seen in some of our CCFs. For instance, the CCF peak in Fig. 8 is steeper on the right hand side. If we subtract a constant from both ME light curves before the *AS* (increasing the *AS* discontinuity, see Fig. 9a) the peak asymmetry becames more prounanced. Instead by subtracting 0.5 *cts s*$^{-1}$ from both ME light curves *after* the *AS* (changing the discontinuity from a step-up to a step-down), then an asymmetric peak, which is steeper on the left hand side, is obtained. This clearly shows that the discontinuities introduced by the *AS* procedure can also make the shape of the CCF peak asymmetric. For observation B, that has no *AS*, the peak is probably due to instability in the background which are then reflected in the background–subtracted source light curves. Indeed if we cross–correlate either one of the source light curves in the two energy bands with the light curve of the background we find a negative peak centered around zero time delay, which indicates an excess of background subtraction.

2.3.   Search for QPOs

We re–analysed the 1–9 keV ME light curves from the observations in Table 1, in order to carry out a detailed search for the QPOs with frequencies of $\sim 1 - 2.5 \times 10^{-3}$ Hz reported by PL. The 120 s binned light curve from each observation was divided in M consecutive intervals of $\sim 1 - 2$ hr duration and the

average power spectrum calculated over the power spectra from individual intervals. This allowed to approximately reproduce the frequency range and resolution used by PL in their analysis. Values of M equal to 23, 17, 8, 10 and 17 were used for observations J, C, I, A–F–G and B–D, respectively. This method of analysis reduces by about one decade the low frequency end of the power spectra, such that only marginal evidence is found for the increase towards low frequencies, that reflects the *red noise* variability of the source. In any case, to search for QPOs we adopted a recently developed technique to detect significant power spectrum peaks even in the presence of "coloured" noise components arising from the source variability (Israel & Stella 1995; Stella et al. 1995). The technique relies upon a suitable smoothing algorithm in order to model the continuum power spectrum components underlying any possible peak. By dividing the power spectrum by the smoothed spectrum, a flat (white noise–like) spectrum is produced, the statistical properties of which are worked out as the ratio of two random variables of know distribution, namely the power spectrum and the smoothed spectrum. A search for oscillations is then carried out by looking for peaks in the divided power spectrum which exceed a given detection threshold.

Selected average spectra and the corresponding 95% confidence detection thresholds are shown in Fig 10. No significant peaks exceeding the threshold were found in the frequency range $\sim 4 \cdot 10^{-4}$ –$4 \cdot 10^{-3}$ Hz for any of the power spectra from observations C, B–D, A–F–G, J and I. Observation J was also analysed in different time intervals, in consideration of the possible malfunctioning of one of the ME detectors during the second half of the observation (see Section 2.2). This was done by calculating a power spectrum for the source light curve and a power spectrum from the corresponding background light curve during each of the 4 array swap–free intervals in between the third array swap and the end of the observations. These power spectra and the corresponding 95% confidence detection thresholds are shown in Fig 11. Significant peaks are clearly detected in the second and fourth power spectra from the source at a frequency of about 1.8 and 2.6×10^{-3} Hz, respectively. It is very likely that these peaks were caused by some kind of quasi–periodic instability in the detector of the first half of the ME array that did not function properly during the second half of observation J. The LE light curves (0.05–2.0 keV), characterized by a poorer signal to noise ratio, were also searched for QPOs; only negative results were found.

Our results argue against the detection of QPOs in the X–ray flux of NGC 5548 reported by PL. The power spectrum technique used by PL involves averaging the logarithm of the power spectra from different intervals therefore producing power estimates that approximately follow a Gaussian distribution (Papadakis & Lawrence 1993b). Model fitting can then be performed using standard least square techniques. The continuum power spectrum components are well fitted by a constant

(representing the counting statistics noise) plus a power law (describing the source red noise). According to PL the grouped power spectra from the three longest observations (C, I and J) display a 95% significant QPO peak (as estimated through an F–test after the addition of a Guassian to the model function). However, we have shown that the QPO during observation J very likely arise from a detector problem.

PL devised also a test to evaluate the significance of power spectrum peaks from individual observations. The best fit model (a power law plus a constant) is used to estimate the continuum components. The power spectrum is then divided by the best fit model in order to produce a white noise power spectrum in which the presence of statistically significant peaks is tested. PL found, in 3 out of 5 cases, a peak in the $1.1 - 2.4 \times 10^{-3}$ Hz frequency range at a significance level of $> 95\%$. However, PL did not take into account the statistical uncertainties introduced in the divided power spectrum by the uncertainties in the best fit model (as evidenced by the lack of any mention of them), therefore overestimating the significance of the peaks. To reassess this significance, we extracted the power spectra from Fig. 1 of PL fitted them with a constant, after excluding the power estimates corresponding to the peaks and the red noise. These constants together with their 1σ uncertainties on these averages, were then used to work out the distribution of the divided spectrum in a way that parallels the method of Israel & Stella (1995). Based on this distribution the significance of the peaks in Fig. 2 of PL was evaluated again. The divided power specta of observations A–F–G (G3 in Table 1 of PL) and observation I are characterised by a peak with a significance of $\sim 95\%$ and $\sim 88\%$, respectively. These values are lower than those worked out by PL ($\sim 98\%$ and $\sim 96\%$, respectively). The power spectrum of observation J, which formally contains the most significant peak, was disregarded in consideration of the detector problem discussed above.

3. Conclusion

Our re–analysis of the CCFs of EXOSAT ME light curves of NGC5548 does not confirm the claim of KB of a ~ 5000 s delay between the medium and soft X–rays variations. This was considered as a strong argument in favour of models where medium energy X–rays are produced by scattering of softer photons. Our results do not exclude this possibility. We note however that the 1990 ROSAT observations (Nandra et al. 1993) detected a variability pattern hardly consistent with very soft X–ray variations (0.1–0.4 keV) preceding the variations of somewhat harder X–rays (1–2.5 keV). This indicates the complexity of physical processes occurring in the source.

Our power spectrum analysis does not confirm the detection of QPOs in the mHz range reported by PL. In particular we have shown that the only power spectrum peak with a significance of $> 95\%$ most probably results from the malfunctioning of one ME detector. The argument of PL according to which the black hole mass of NGC 5548 has an embarrassingly low value of a few hundred thousand solar masses, loses its validity.

While the results of this paper are essentially "negative", we hope that our work contribute illustrating subtle effects which may yield spurious results in the analysis of X–ray light curves from AGNs.

Table 1

Obs	Date	Me exp. (s)	rms disp. $cts\ s^{-1}$	expe. rms $cts\ s^{-1}$	No. of AS	Counts $cts\ s^{-1}$	Al/P (s)	Bor (s)	3Lex (s)
A	84/032	17010	0.23	0.27	0	3.32±0.18	1902	7153	3202
B	84/062	32630	0.26	0.20	0	4.44±0.04	3483	3679	2763
C	84/193	59430	0.26	0.27	3	2.88±0.03	11872	26488	11053
D	85/062	26800	0.22	0.20	1	3.65±0.04	4434	11413	4605
E	85/159	25750	0.30	0.26	1	1.43±0.05	6675	9915	3824
F	85/173	17020	0.30	0.20	2	3.03±0.05	4252	6672	3311
G	85/186	23370	0.34	0.20	1	1.82±0.04	3613	10963	3095
H	85/195	19020	0.22	0.19	1	1.35±0.05	4040		2622
I	86/019	59860	0.39	0.22	3	4.97±0.02		3469	39037
J	86/062	83830	0.45	0.29	6	3.82±0.02	2392	4017	69809

REFERENCES

Clavel, J., et al. 1991, ApJ, 366, 64.

Clavel, J., et al. 1992, ApJ, 393,113.

De Korte, P. A. J., et al. 1981, Space Sci.Rev., 30, 495.

Done, C., Pounds, K. A., Nandra, K., & Fabian, A. 1995, MNRAS, in press.

Edelson, R. A., & Krolik. J. H. 1988, ApJ, 333, 646.

Giommi, P., Barr, P., Garilli, B., Gioia, I.M., Maccacaro, T., Maccagni, D., Schild, R.E., 1987, ApJ, 322, 662

Grandi, P., Tagliaferri, G., Giommi, P., Barr, P., Palumbo, G.C. 1992, ApJS, 82, 93.

Green, A. R., Mc Hardy, I. M., & Lehto, H. J. 1993, MNRAS, 265, 664.

Haardt, F., & Maraschi, L. 1993, ApJ, 413, 507.

Kaastra, J. S., Barr, P. 1989, A&A, 226, 59.

Korista K. T., et al. 1995, ApJS, 97, 285.

Israel, G. L. & Stella, L. 1995, submitted to ApJ.

Molendi, S., Maraschi, L., Stella, L. 1992, MNRAS, 255, 27

Mushotzky, R. F., Done, C., & Pounds, K. A. 1993, ARA&A31, 717.

Nandra, K., Pounds, K. A., Stewart, G. C., George, I. M., Hayashida, K., Makino, F., & Ohashi, T. 1991, MNRAS, 248, 760.

Nandra, K., et al 1993, MNRAS, 260, 504.

Papadakis, I. E., & Lawrence, A. 1993a, Nature, 361, 233.

Papadakis, I. E., & Lawrence, A. 1993b, MNRAS, 261, 612.

Parmar, A.N., & Izzo, C., 1986, The EXOSAT Express, no. 16, p. 21.

Stella, L., & Angelini L. 1992, in "Data Analysis in Astronomy IV", Eds. V. Di Gesù, L. Scarsi, R. Buccheri, P. Crane, M.C. Maccarone & H.V. Zimmerman, (Plenum Press: New York), p. 59.

Stella, L., Arlandi, E., Tagliaferri, G., & Israel, G. L. 1995 in "Time Series Analysis in Meterology and Astronomy", ed. S. Rao, in press.

Tagliaferri, G., Stella, L., Maraschi, L, Treves, A., & Celotti, A. 1991, ApJ, 380, 78.

Walter, R., & Courvoisier, T. 1990, A&A, 233, 40.

Walter, R., Courvoisier, T., Done, C., Maraschi, L., Pounds, K., & Urry, M. 1995, preprint.

White, N. E., Peacock, A. 1988, in "X-ray Astronomy with EXOSAT", eds. R. Pallavicini & N. E. White, p. 7.

Życki, P. T., Krolik, J. H., Zdziarski, A. A., & Kallman, T. R. 1994, ApJ, 437, 597.

Figure captions

Figure 1: NGC5548 LE (0.05–2 keV) and ME (1–4 and 4–9 keV) light curves during the longest EXOSAT observation (1986/062, observation J through the paper). The arrows show the array swaps of the ME detector halves, the corrspective data gaps of about 15 minutes are filled with the running mean (see text). Note the big gap at the beginning due to the switch off of the detectors at the satellite perigee passage.

Figure 2: LE/ME light curve cross correlations of observation J. All data shown in Fig. 1 has been used. Note that the peak centered around a delay of $\sim 7 - 8$ ks is also clearly asymmetric.

Figure 3: LE/ME (panel a) and ME/ME (panel b) light curve cross correlations of observation J. A clear peak around zero time lag is clearly present in both cases. The Gaussian plus constant model fit to the central peak is also shown. The fit was carried out over a range of lags of ±40 ks and ±20 ks respectively. In the ME/ME case, a linear term was added to the fit, in order to account for the CCF asymmetry.

Figure 4: cross correlations of the light curves of observation J divided in three different segments (see text). A clear peak is present only in the third part (panels e–f).

Figure 5: top panel: final part of the ME light curves of observation J, the arrows show the array swaps of the ME detector halves. Note the noisier light curves before and after the first and last array swap. Bottom panel the same light curves after having added 0.1 and 0.4 $cts\ s^{-1}$ to the central 1–4 and 4–9 keV light curves respectively; the discontinuity due to the detector array swaps is clearly reduced.

Figure 6: cross correlations of the ME light curves of observation I. Again a strong peak centered on zero delay is clearly present.

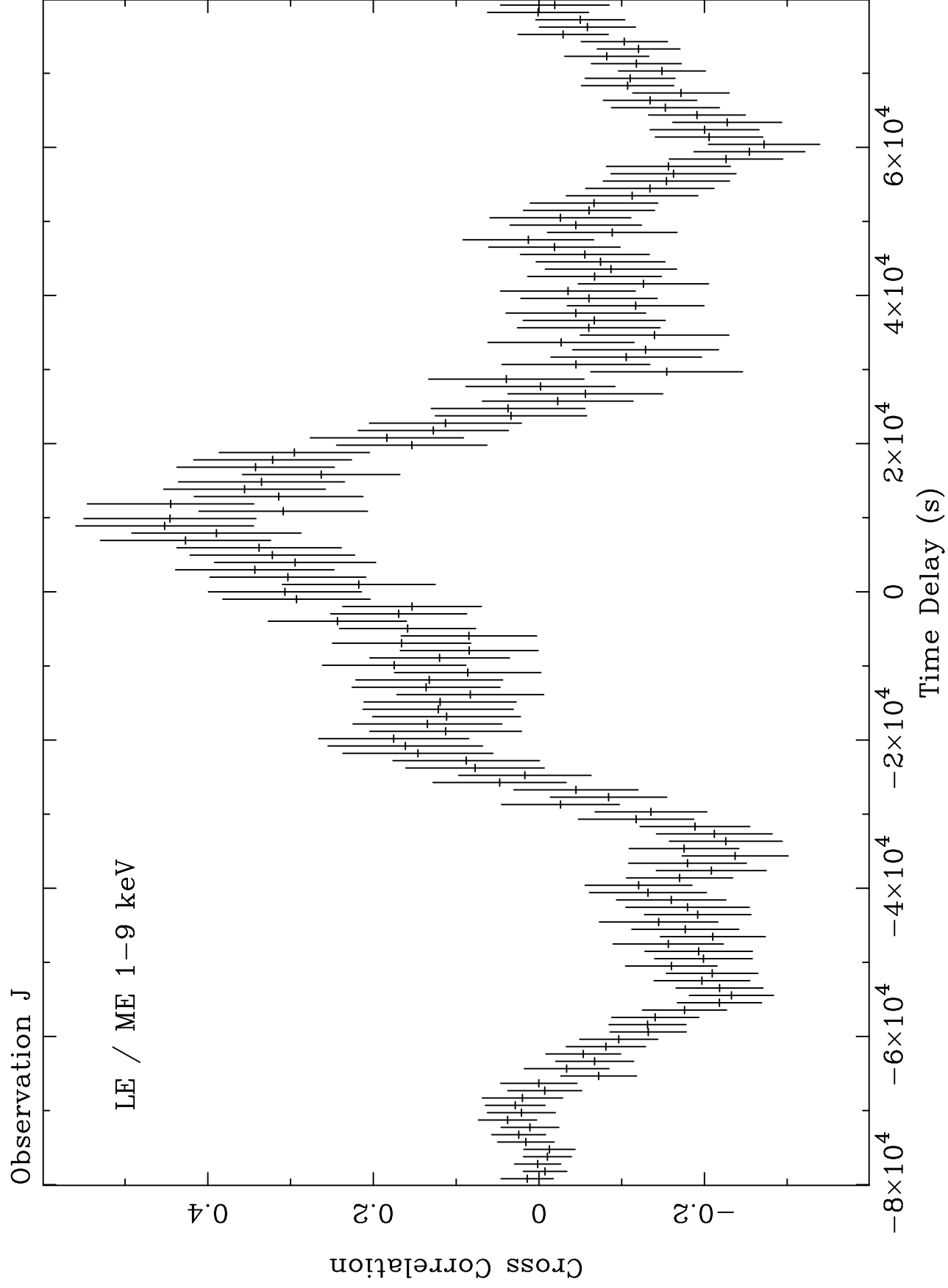**Figure 7:** cross correlations of the ME light curves of observation B. The peak is not consistent with zero delay time, and would imply that the variations in the 1–4 keV light curve precede the variations in the 4–9 keV light curve. However this result is probably spurious, see text.

Figure 8: cross correlations of the ME light curves of observation G. The peak is not consistent with zero delay time, and would imply that the variations in the

1–4 keV light curve precede the variations in the 4–9 keV light curve. However this result is probably spurious, see text.

Figure 9: top panel: ME light curves of observation G, the arrows show the array swap of the ME detector halves. Bottom panel: the same light curves after having added 0.2 cts s^{-1} to the two light curves before the array swap; the discontinuity due to the detector array swap is clearly reduced.
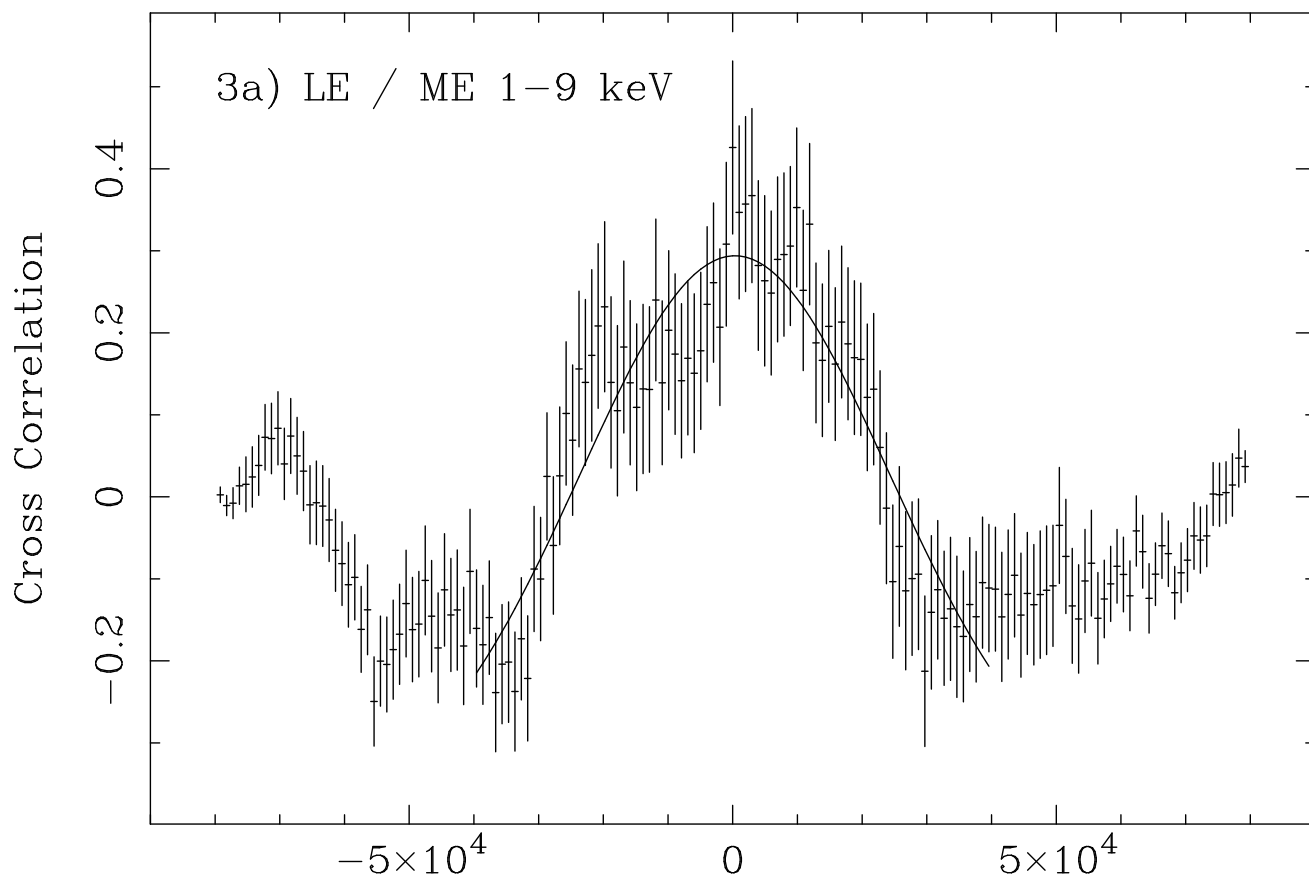
Figure 10: Power spectra from the EXOSAT ME 1–9 keV light curves of observations A–F–G (84/032, 85/173 and 85/186), B–D (84/062 and 85/062), C (84/193), and I (86/019) (from top to bottom); the solid lines give the corresponding 95% confidence detection thresholds.

Figure 11: EXOSAT ME 1–9 keV Power spectra of the ME light curves of NGC 5548 (left) and the background (right) during the second half of observation J. Each panel refers to an array swap free interval, starting from the third array swap (see text for details). The ME array half used in each panel is indicated. The solid lines give the 95% confidence detection thresholds.
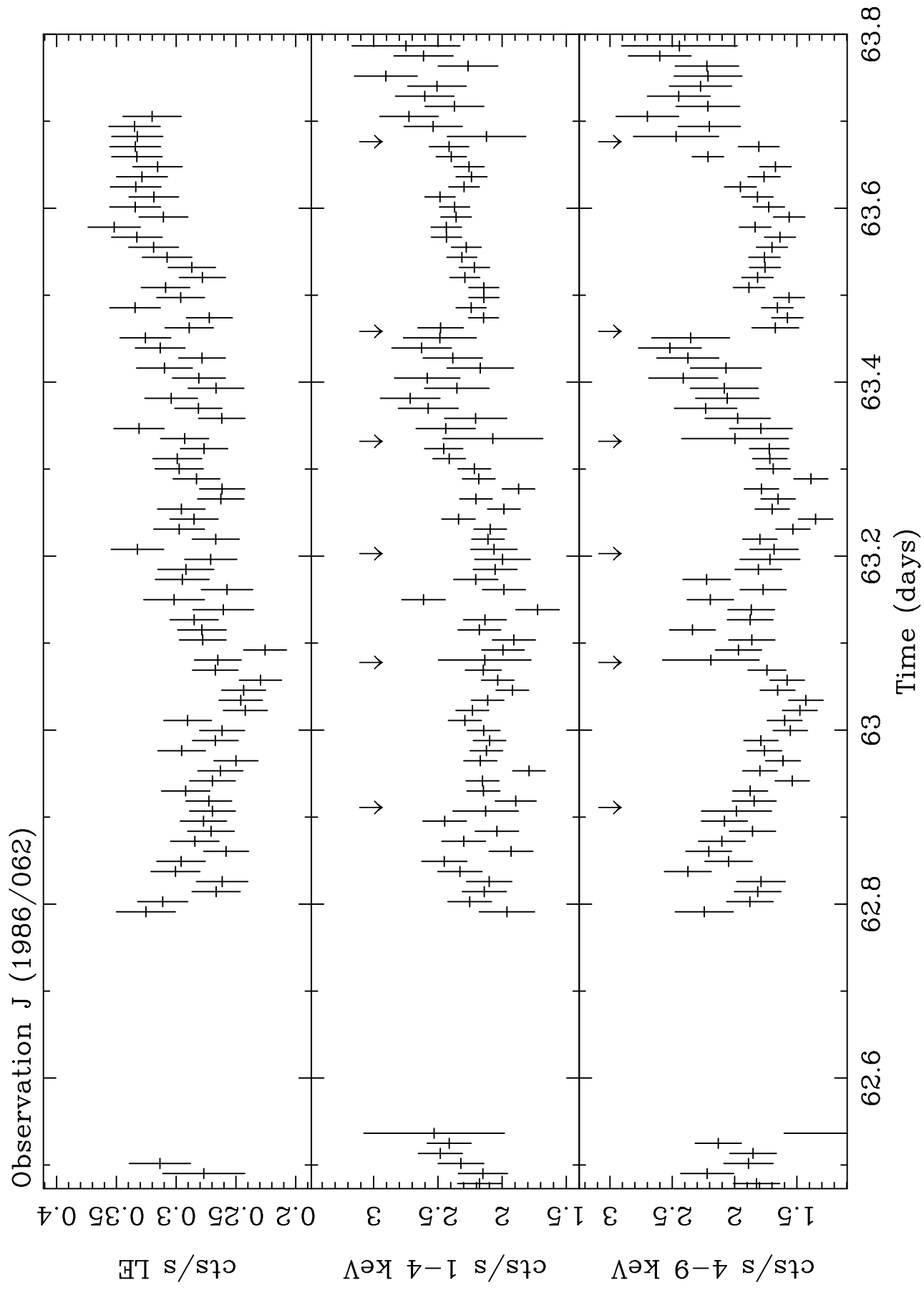
Observation J (1986/062)

Time (days)

cts/s LE

cts/s 1−4 keV

cts/s 4−9 keV

Observation J

LE / ME 1−9 keV

Observation J

3a) LE / ME 1−9 keV

Cross Correlation

−5×10⁴ 0 5×10⁴

Observation J

3b) ME 1−4 keV / 4−9 keV

Cross Correlation

−5×10⁴ 0 5×10⁴

Time Delay (s)

Observation J, first part

4a) LE / ME 1–9 keV

Observation J, first part

4b) ME 1–4 keV / 4–9 keV

Observation J, second part

4c) LE / ME 1–9 keV

Observation J, second part

4d) ME 1–4 keV / 4–9 keV

Observation J, third part

4e) LE / ME 1–9 keV

Observation J, third part

4f) ME 1–4 keV / 4–9 keV

Time Delay (s)
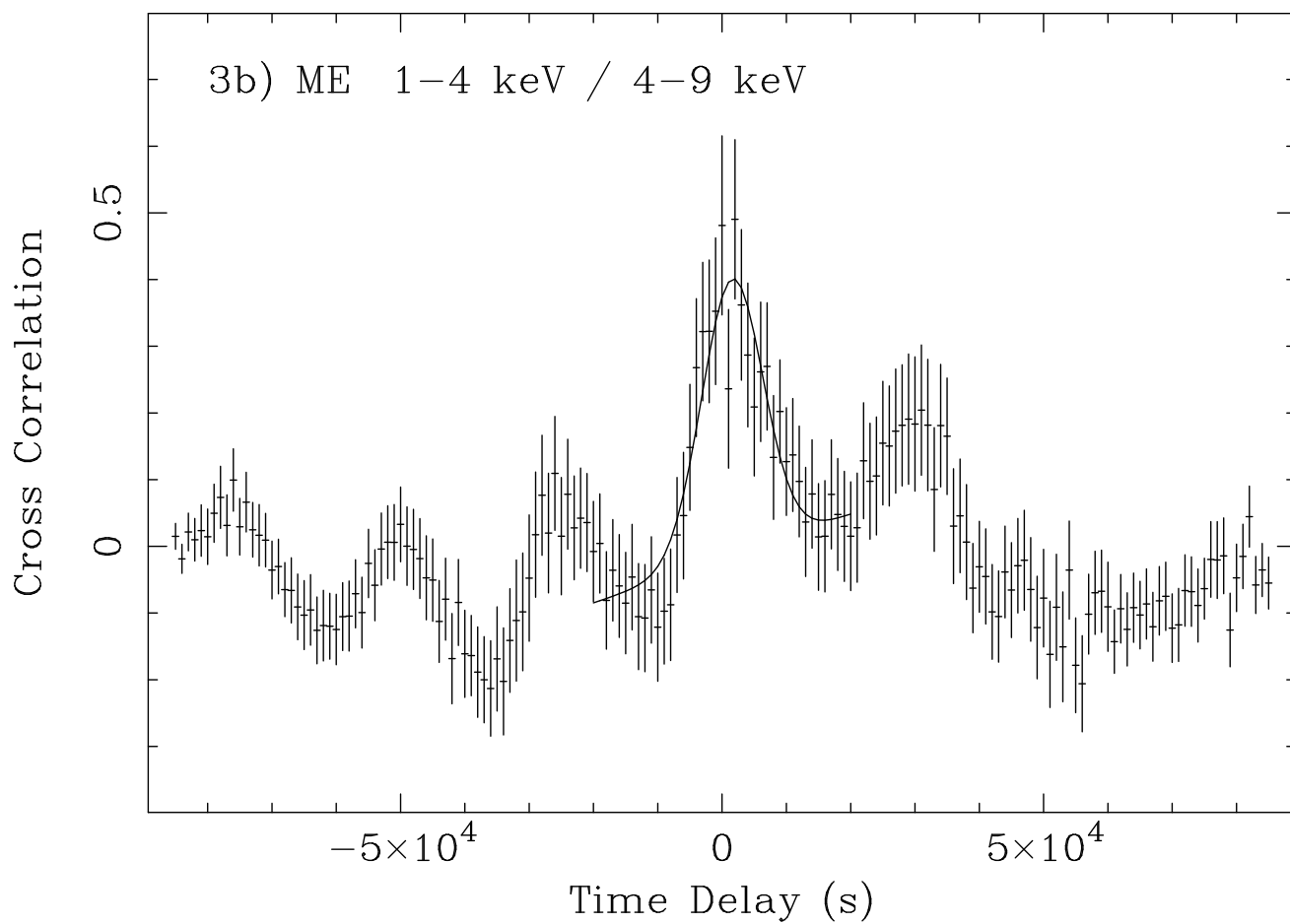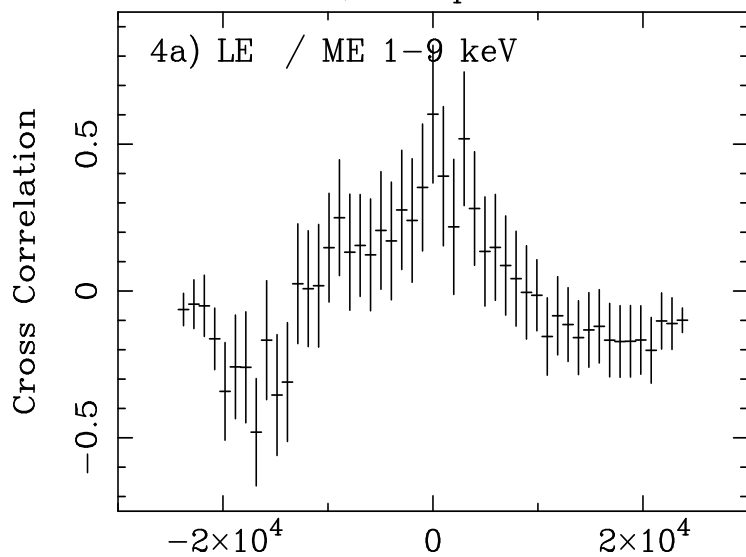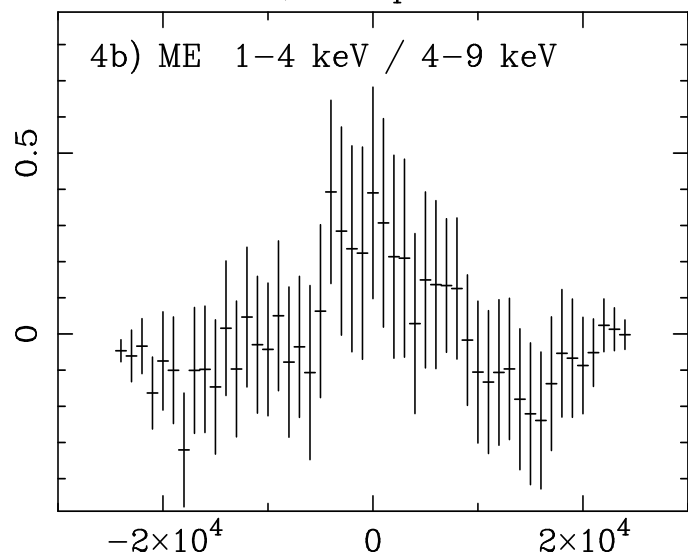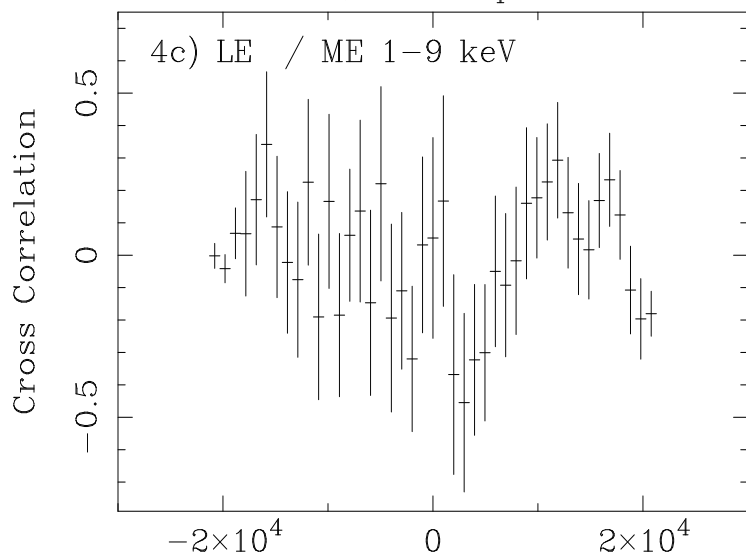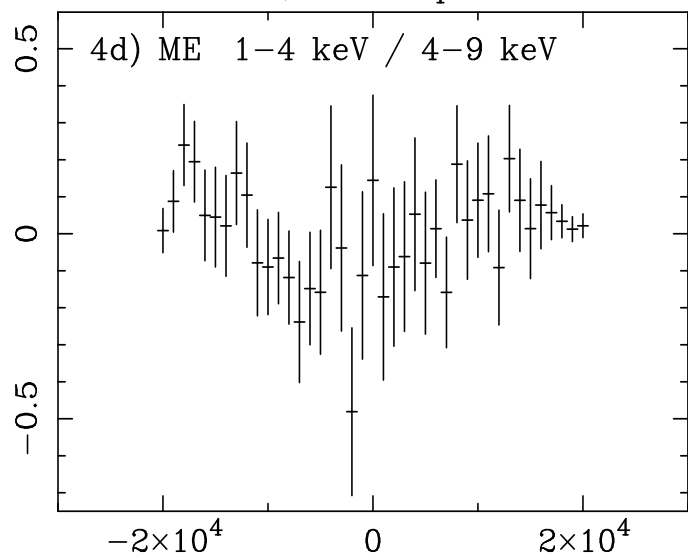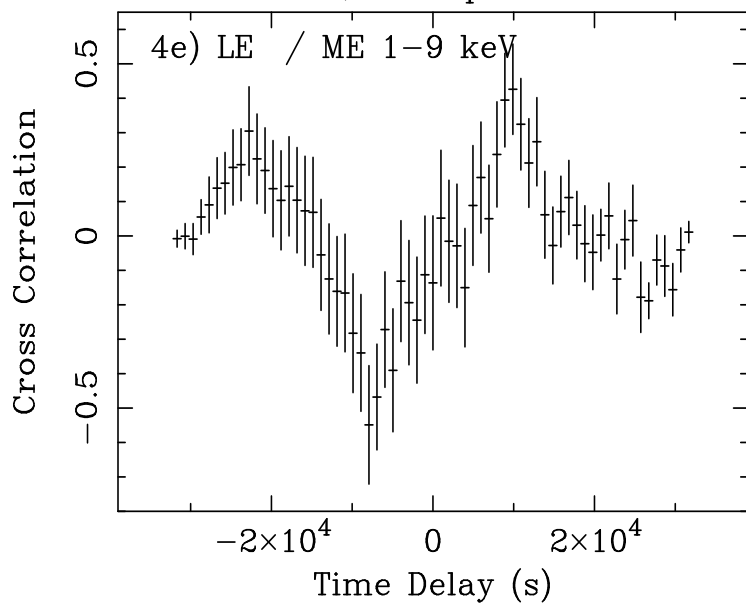
Observation J, third part

Observation J, third part

+ 0.1 cts/s

+ 0.4 cts/s

Observation I

ME 1–4 keV / ME 4–9 keV
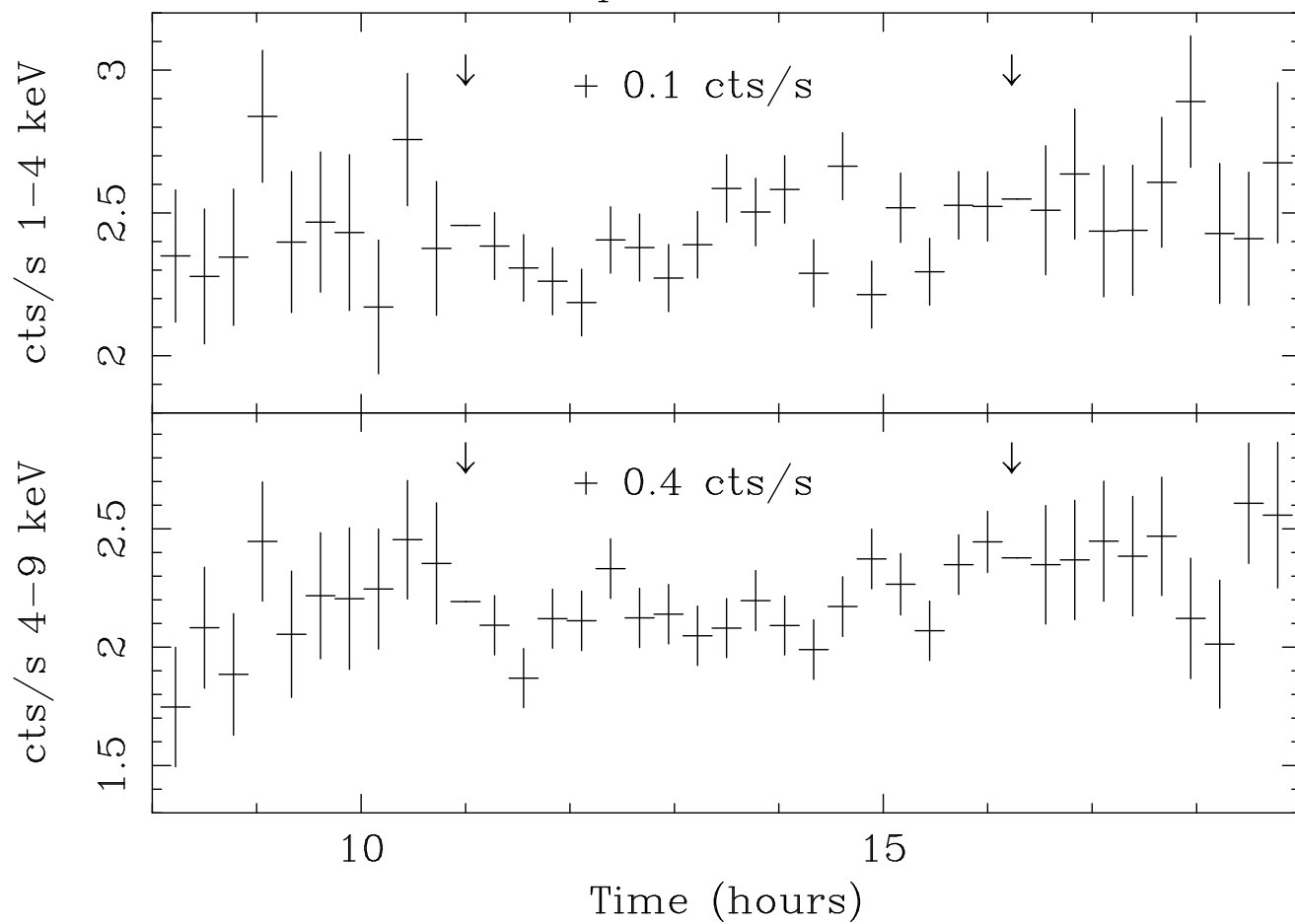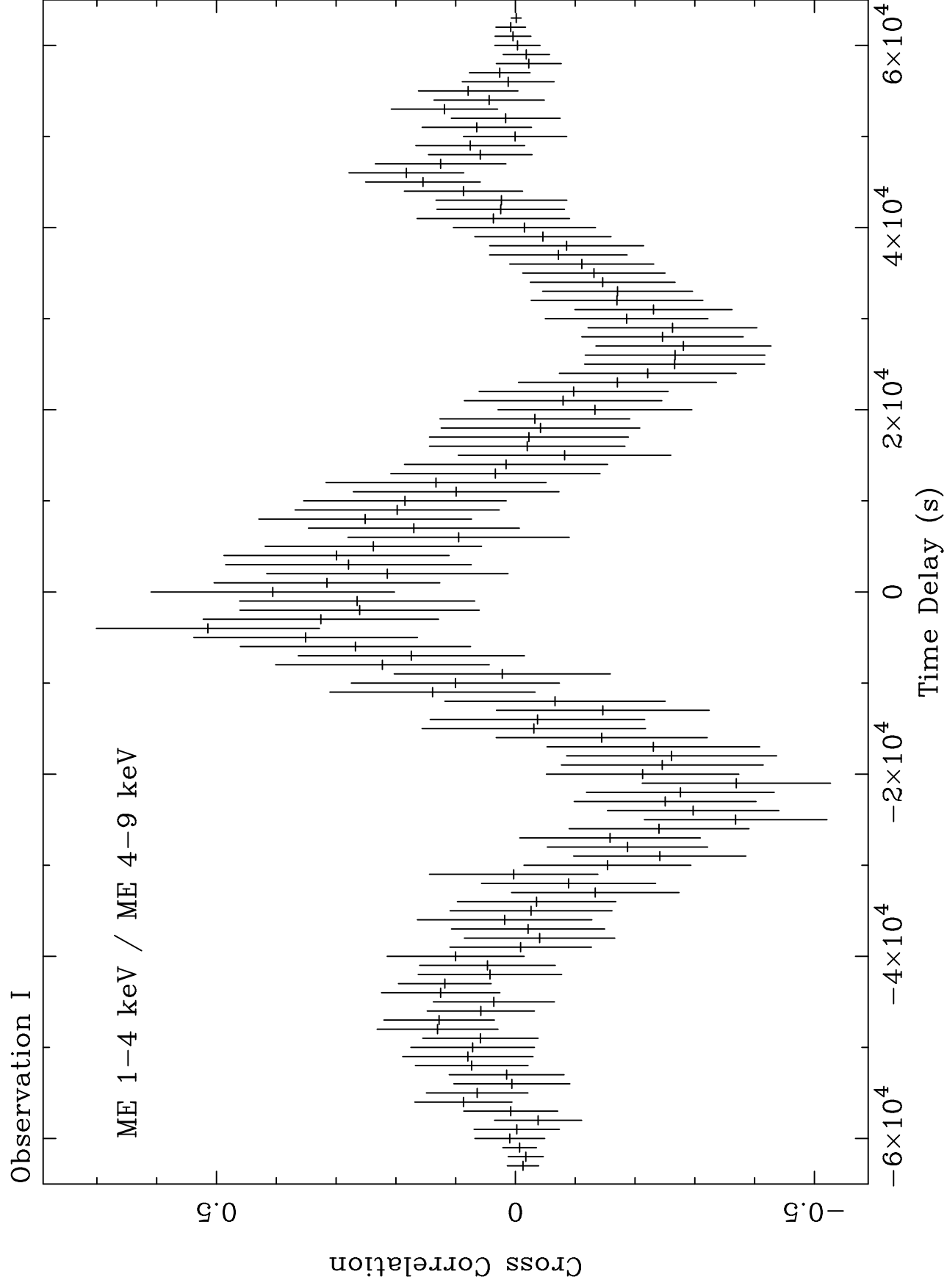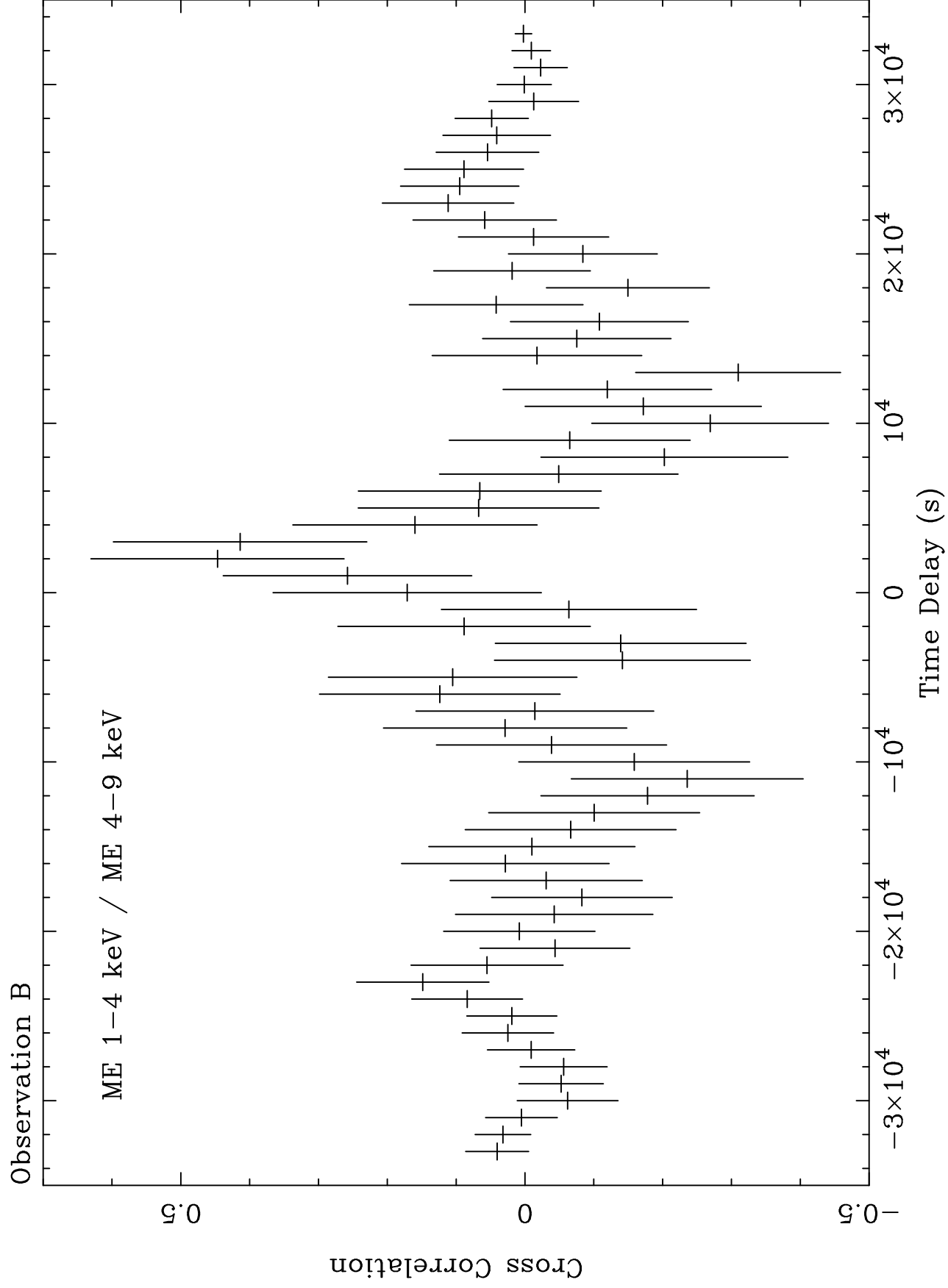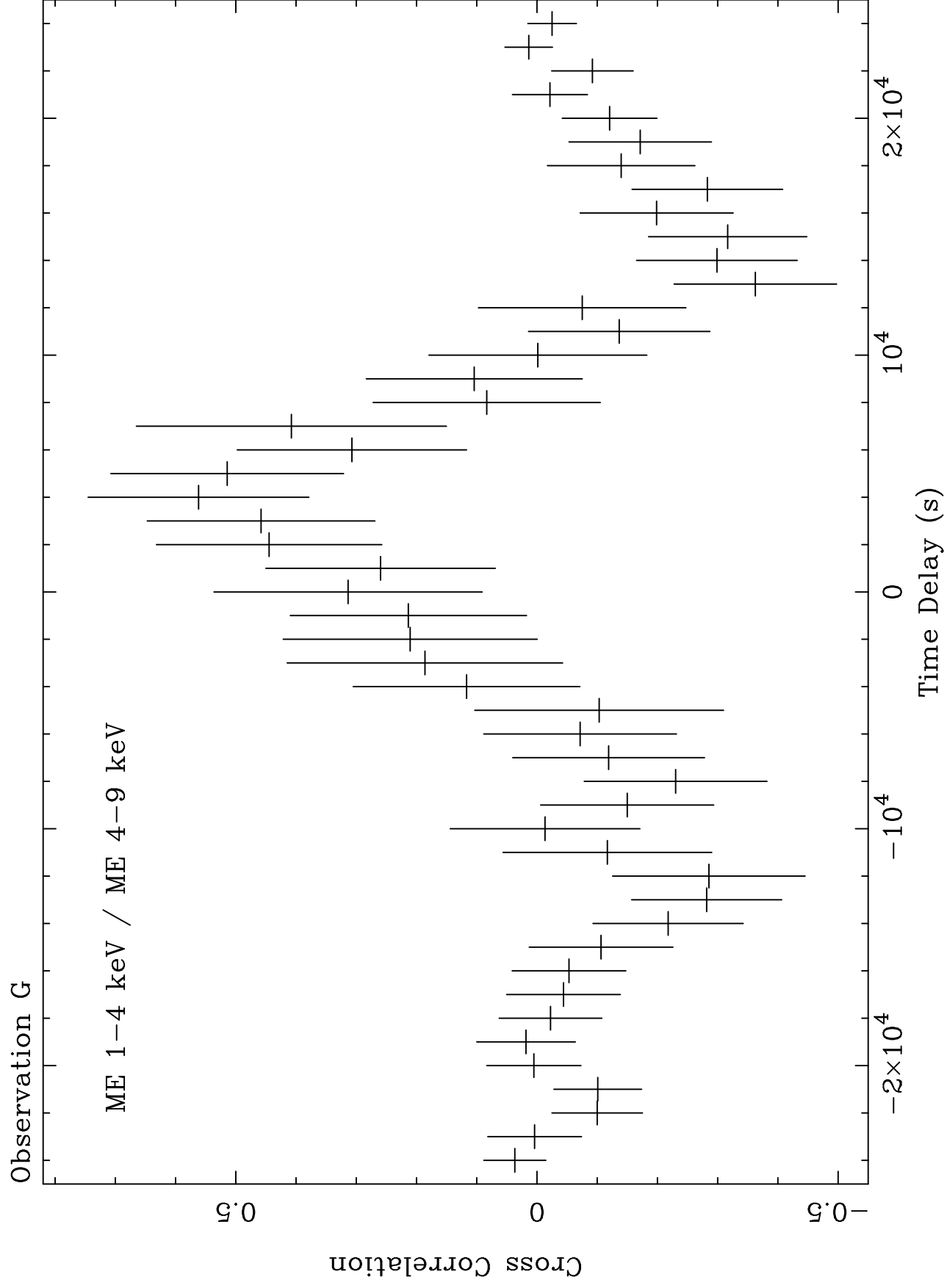
Observation G

Observation G

EXOSAT ME   1-9 keV

A-F-G

B-D

C

I

Power

Frequency (Hz)

10^{-3}
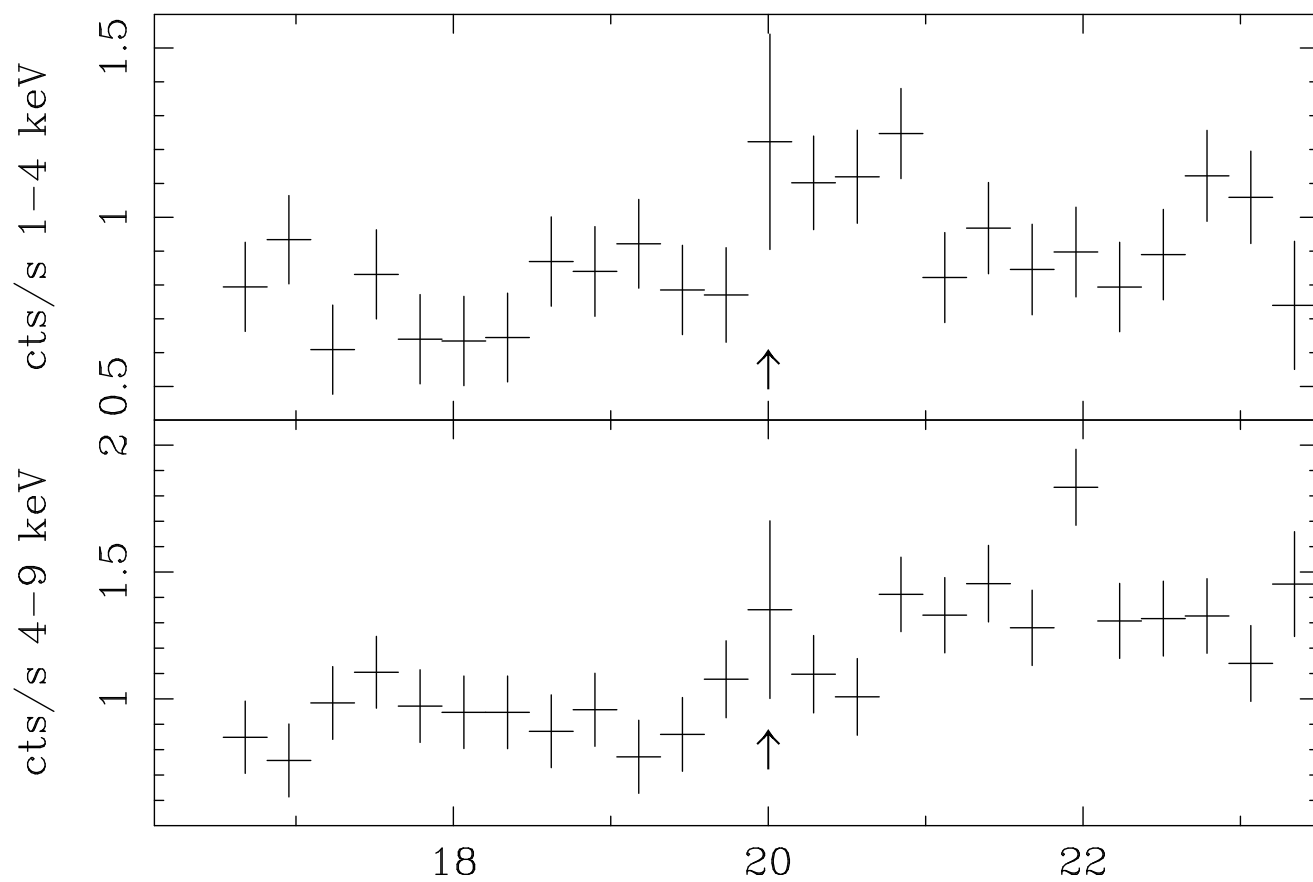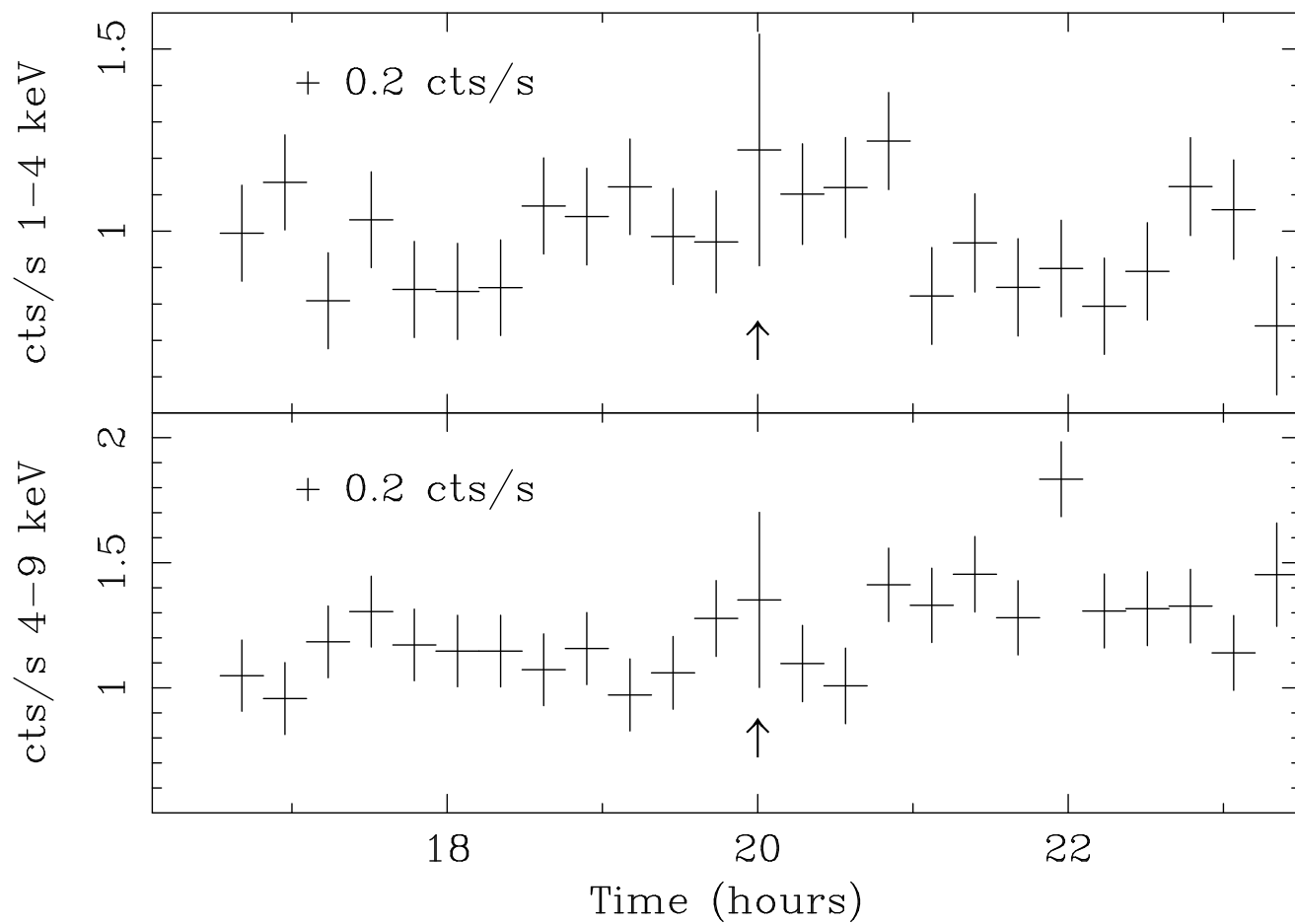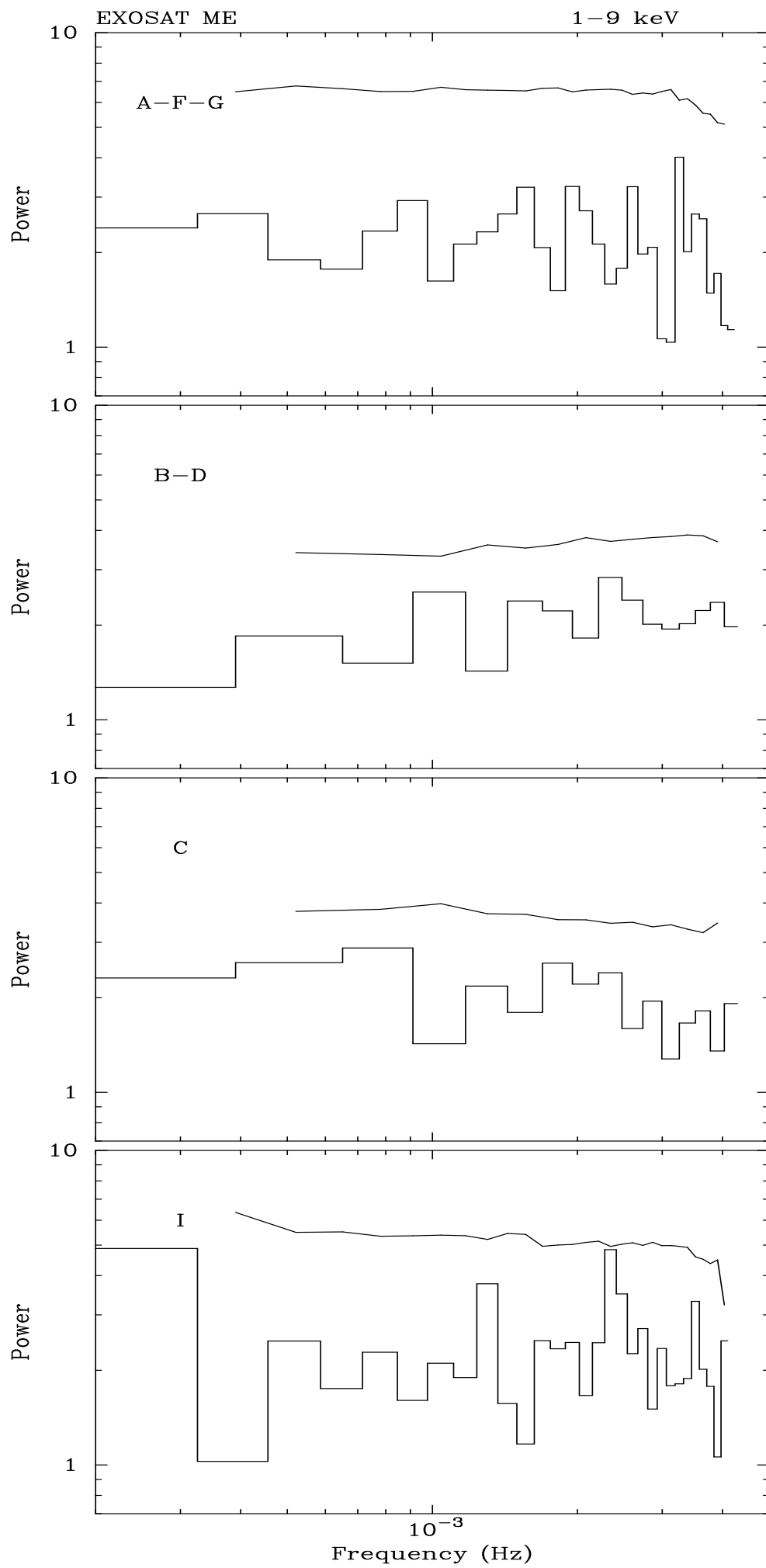
NGC 5548 (Source)

NGC 5548 (BG)